

Search for leptoquarks and other new particles with lepton-hadron signature in $e^+ e^-$ interactions

JADE Collaboration

W. Bartel, L. Becker, R. Felst, D. Haidt, G. Knies, H. Krehbiel, P. Laurikainen¹, N. Magnussen²,
R. Meinke, B. Naroska, J. Olsson, D. Schmidt², P. Steffen
Deutsches Elektronen-Synchrotron DESY, D-2000 Hamburg, Federal Republic of Germany

T. Greenshaw, J. Hagemann, G. Heinzelmann, H. Kado, C. Kleinwort, M. Kuhlen, A. Petersen³,
R. Ramcke, U. Schneekloth⁴, G. Weber
II. Institut für Experimentalphysik der Universität Hamburg, D-2000 Hamburg, Federal Republic of Germany

K. Ambrus, S. Bethke⁵, A. Dieckmann, G. Eckerlin, E. Elsen, J. Heintze, K.-H. Hellenbrandt,
S. Komamiya³, J. van Krogh, H. Rieseberg, H. v.d. Schmidt, L. Smolik, J. Spitzer, A., Wagner, M. Zimmer
Physikalisches Institut der Universität Heidelberg, D-6900 Heidelberg, Federal Republic of Germany

C.K. Bowdery, A.J. Finch, F. Foster, G. Hughes, J.M. Nye, I.W. Walker
University of Lancaster, Lancaster LA1 4YB, UK

J. Allison, R.J. Barlow, J. Chrin, I.P. Duerdoth, F.K. Loebinger, A.A. Macbeth, H.E. Mills⁶, P.G. Murphy,
K. Stephens, P. Warming⁷
University of Manchester, Manchester M13 9PL, UK

R.G. Glasser, P. Hill, J.A.J. Skard, S.R. Wagner⁸, G.T. Zorn
University of Maryland, College Park, MD20742, USA

S.L. Cartwright⁴, D. Clarke, R. Marshall, R.P. Middleton
Rutherford Appleton Laboratory, Chilton, Didcot OX11 0QX, UK

T. Kawamoto, T. Kobayashi, M. Minowa, H. Takeda, S. Yamada
International Center for Elementary Particle Physics, University of Tokyo, Tokyo, Japan

Received 27 April 1987

Abstract. Using the JADE detector at PETRA, a search for hadronic events with isolated leptons in $e^+ e^-$ annihilation was performed. No evidence was found for the production of leptoquarks or color octet

leptons and mass limits were obtained. Three hadronic events, each of them with two isolated muons, were detected and found to be in agreement with predictions of the α^4 QED process $e^+ e^- \rightarrow q\bar{q}\mu^+\mu^-$. At the highest PETRA energies, $46.30 \text{ GeV} \leq \sqrt{s} \leq 46.78 \text{ GeV}$, five events with low thrust, $T < 0.8$, and a muon at a large angle with respect to the thrust axis, $|\cos \delta| < 0.7$, were observed. The number of such events expected from an extrapolation of control data at lower energies is 0.56 ± 0.18 . No satisfactory explanation for the excess in terms of background could

¹ University of Helsinki, Helsinki, Finland

² Universität-Gesamthochschule Wuppertal, Wuppertal, FRG

³ Now at SLAC, Stanford, California, USA

⁴ Now at MIT, Cambridge, Massachusetts, USA

⁵ Now at LBL, Berkeley, California, USA

⁶ Now at SCS, Hamburg, FRG

⁷ Now at Digitec, Hamburg, FRG

⁸ Now at University of Colorado, Boulder, Colorado, USA

be found. A corresponding excess of electron events was not seen.

1 Introduction

In this paper we report on a study of the reaction $e^+e^- \rightarrow \mu^+\mu^- + \text{hadrons}$ and on a search for leptons and color octet leptons in e^+e^- annihilation. Three different event topologies are discussed: two acoplanar jets, a muon+jets+missing energy and two muons+jets. Finally we describe an investigation of hadronic events with low thrust containing isolated leptons, for which the Mark J group observed an unexpected behaviour at the highest PETRA energies [1].

2 Event selection and lepton identification

2.1 Event selection

The data were collected with the JADE detector [2] at the PETRA e^+e^- storage ring. Multiparticle events were selected using the criteria described in [3], which are the basis for the selection of multihadronic events in JADE. The most important cuts are:

1. The total lead glass energy in the barrel part of the detector is required to exceed 3 GeV or the energy deposition in each of the endcaps has to be larger than 0.4 GeV.
2. At least four charged particles are demanded to originate from the event vertex.
3. Remaining cosmic ray events, τ -pairs and purely leptonic QED events are removed by visual inspection.

Further cuts, in visible energy $E_{\text{vis}} = \sum_i p_i$ and longitudinal momentum balance $p_{\text{bal}} = \sum_i p_i^z / E_{\text{vis}}$, extract the multihadronic annihilation events from this sample. The sums run over all particle momenta p_i , p_i^z denoting the components along the beam axis.

4. $E_{\text{vis}} > E_b$, where E_b is the beam energy.
5. $|p_{\text{bal}}| < 0.4$.

2.2 Muon identification

Muons are identified as penetrating particles in the muon filter [4], which consists of four successive blocks of absorber material interleaved with layers of drift chambers. It covers 92% of the full solid angle and presents in total at least 6.4 nuclear absorption lengths to particles with incidence perpendicular to the beam. All tracks recorded in the jet chamber are extrapolated through the muon filter, and their likelihood of being muons is tested. The following samples

of tracks are considered as muon candidates in the analysis [5]:

“*Muon candidates*”. At least two hits in the muon chambers outside the magnet yoke are asked for within a 2σ range of the extrapolation of a track taking into account fitting errors and multiple scattering. One missing hit in the 2σ range is permitted, except in the case of the outermost intersected layer of chambers, where a hit has to be present.

“*Good muons*”. Further requirements define the “good muons” used in the analysis. The segmented muon filter enables different selection criteria to be chosen, depending on the goals of the physics analysis. Usually loose cuts are used for new particle searches, where high detection efficiency is essential (see for example [6]), while tight cuts give the cleanest muon sample and are used where the properties to be studied are obscured by a large background, for example for the determination of the semi-muonic branching ratios and fragmentation functions of heavy quarks [7]. The “loose” cuts and the “tight” cuts are defined as follows*.

“*Loose*” cuts. In addition to the above criteria, the track momentum has to exceed 1.8 GeV, the track is required to penetrate more than 4.8 absorption lengths to the outermost associated hit in the muon filter and the χ^2 probability that the jet chamber track matches the μ filter hits has to be greater than 1%.

“*Tight*” cuts. As a further condition there must be no expected hit missing in the muon chambers, and more than 5.8 absorption lengths have to be traversed. At least 3 layers of muon chambers outside the yoke are required to have registered hits which can be associated with the jet chamber track.

2.3 Electron identification

Electrons are identified by their energy loss in the gas of the drift chamber and by their electromagnetic shower detected in the lead glass calorimeter. In order to confine the shower to the central part of the lead glass system which has the highest resolution, an acceptance cut of $|\cos \theta| < 0.76$ is imposed, θ being the angle of the particle with the beam axis.

For a particle to be considered an electron candidate the track momentum has to be greater than 1 GeV, and its energy loss as measured in the jet chamber is demanded to agree with the expectation

* The “loose” cuts correspond to muons of “quality A” and the “tight” cuts to muons of “quality C” in [5]

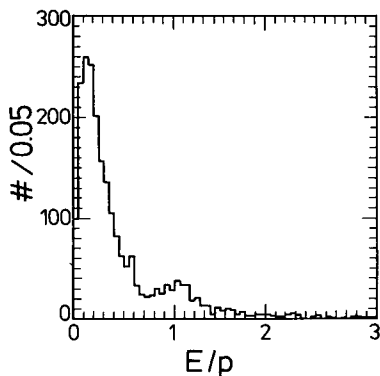


Fig. 1. E/p distribution after dE/dx cut

for electrons within $-1.5\sigma < (dE/dx)_{\text{measured}} - (dE/dx)_{\text{electron}} < +2.0\sigma$. The shape of the lead glass cluster associated with the track is required to be consistent with an electromagnetic shower. An electron candidate is removed if it can be combined with another track to form a photon conversion pair. Finally, the deposited energy E in the leadglass has to agree with the track momentum p , it being required that $0.8 < E/p < 3.0$. Fig. 1 shows the E/p distribution after all except the last of these cuts. There is a distinct electron peak at $E/p=1$.

3 The reaction $e^+ e^- \rightarrow q\bar{q}\mu^+\mu^-$

The process $e^+ e^- \rightarrow q\bar{q}\mu^+\mu^-$ is an α^4 QED process. It is a source of events with isolated energetic muons, and can thus be used to check the sensitivity of the detector to such processes and to study the background for the event topologies to be searched for in the following chapters.

Three classes of Feynman graphs, which are displayed in Fig. 2, contribute to this process. The cross section was calculated using the formalism and computer code developed by Berends, Daverfeldt and

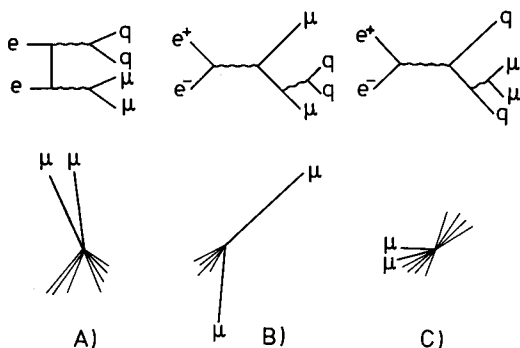


Fig. 2A–C. Feynman graphs and corresponding event topologies for $e^+ e^- \rightarrow q\bar{q}\mu^+\mu^-$

Kleiss [8]. The $q\bar{q}\mu^+\mu^-$ events generated by this program were fragmented according to the Lund scheme [9] and passed through the detector simulation and analysis chain in order to determine the detection efficiency. The selection criteria, optimized with respect to the 2-photon conversion diagrams (Fig. 2A) which give the main contribution to the total cross section, were as follows:

1. The event had to fulfill the multihadron selection requirements.
2. 2 “muon candidates” with $p_\mu > 3$ GeV, at least one of them being a “good muon” (“loose” cuts) were asked for.
3. No additional charged tracks, with the exception of other “muon candidates”, were allowed in cones with a half opening angle of 60° surrounding each of the two muons.
4. It was required that there be less than 1 GeV lead glass energy in these cones.
5. The remaining events were scanned by a physicist, and it was required that there be two clearly separated tracks visible within the muon filter.

Data corresponding to an integrated luminosity of 94.2 pb^{-1} at centre of mass energies ranging from 29.5 to 46.78 GeV were analysed. Three events were found after cuts, as compared to 1.2 events expected from the QED simulation of $e^+ e^- \rightarrow q\bar{q}\mu^+\mu^-$. The background, mainly from $\mu\mu\tau\tau$ and $q\bar{q}$ events with fake muons, was estimated to be less than 0.3 events. In Fig. 3 the muon opening angles and hadronic invariant masses are compared to the QED distribu-

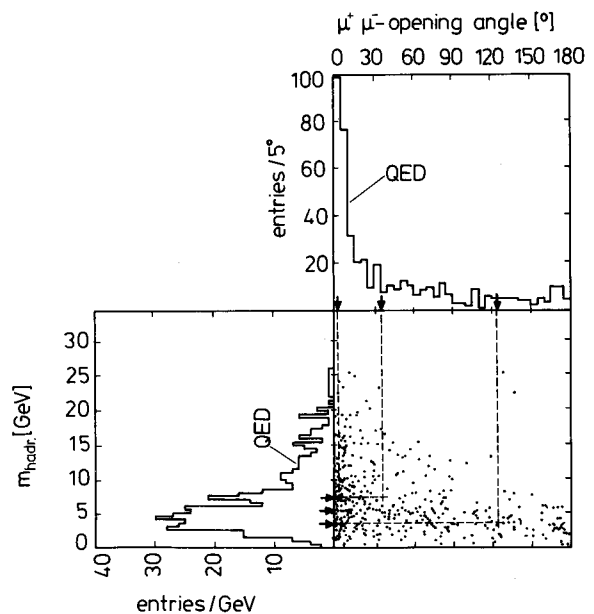


Fig. 3. Muon opening angle and hadronic invariant mass for simulated $q\bar{q}\mu^+\mu^-$ events after cuts. The measured values of the three observed events are indicated

tions. Within the limited statistics, event rate and kinematic configurations agree with the QED expectation. The observation of these events at the expected rate gives confidence that the JADE detector is capable of detecting rare events with isolated muons.

4 Leptoquarks

4.1 Introduction

Light leptoquark bosons with charge $1/3, 2/3, \dots$, which decay into a quark and a lepton, appear in several technicolor and composite models [10, 11]. In the present analysis emphasis is placed on a specific model due to B. and F. Schrempp [10] with second generation leptoquarks of charge $2/3$. In this model second generation quantum number is conserved. Thus a second generation leptoquark χ_μ can only decay into either $c\bar{\nu}_\mu$ or $s\mu^+$.

The cross section for pair production of charged color triplet spinless bosons in e^+e^- annihilation is

$$\frac{d\sigma}{d\Omega}(e^+e^- \rightarrow \chi\bar{\chi}) = 3 \cdot \frac{\alpha^2}{8s} \cdot Q^2 \cdot \beta^3 \cdot \sin^2\theta \quad (1)$$

where $\beta = \sqrt{1 - 4m_\chi^2/s}$, m_χ is the leptoquark mass, $Q = 2/3$ and θ is the production angle with respect to the beam direction. The cross section rises slowly from threshold with increasing energy, due to the β^3 factor. Near threshold the contribution to the total hadronic cross section is too small to be measurable, but leptoquarks can be searched for by their distinctive event topologies (see Fig. 4):

- A) $e^+e^- \rightarrow \chi_\mu\bar{\chi}_\mu \rightarrow c\bar{\nu}_\mu\bar{c}\nu_\mu$: two acoplanar jets.
- B) $e^+e^- \rightarrow \chi_\mu\bar{\chi}_\mu \rightarrow c\bar{\nu}_\mu\bar{s}\mu^-$ or *c.c.*: two jets, a muon and missing momentum.
- C) $e^+e^- \rightarrow \chi_\mu\bar{\chi}_\mu \rightarrow s\mu^+\bar{s}\mu^-$: two jets and two muons.

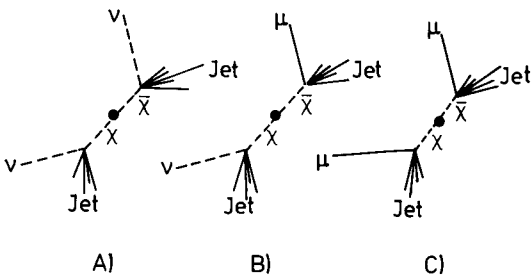


Fig. 4A–C. Event topologies for leptoquarks

Using a Monte Carlo simulation of leptoquark events, methods of isolating them from ordinary events by applying certain cuts were developed. The detection efficiencies after the cuts were also obtained from the simulation. The leptoquarks were fragmented like heavy quarks using the Lund model [9] and the Peterson fragmentation function [12].

Events of classes A), B) and C) were searched for in the high energy data sample corresponding to an integrated luminosity of 24.5 pb^{-1} between $\sqrt{s} = 38.66$ and 46.78 GeV .

4.2 Analysis

A) *Acoplanar jets*. Cuts identical to those used in the searches for the supersymmetric partner of the Z^0 [13] and monojet events [14] previously performed by JADE were applied to the multiparticle events defined in Sect. 2.1. These were:

1. $2/5 < E_{\text{vis}}/\sqrt{s} < 1$.
2. $|\cos\theta_T| < 0.65$, with θ_T the angle between thrust axis and the positron beam direction.
3. $\phi_{\text{acop}} > 40^\circ \cdot (1 + |\cos\theta_T|)$.

The acoplanarity angle ϕ_{acop} is given by

$$\phi_{\text{acop}} = \arccos\left(-\frac{(\mathbf{p}_+ \times \mathbf{n}_z) \cdot (\mathbf{p}_- \times \mathbf{n}_z)}{|\mathbf{p}_+ \times \mathbf{n}_z| \cdot |\mathbf{p}_- \times \mathbf{n}_z|}\right) \quad (2)$$

where \mathbf{p}_+ and \mathbf{p}_- are defined as follows: Each event is split into two halves using a plane perpendicular to the thrust axis. \mathbf{p}_+ and \mathbf{p}_- are then the sums of the momenta of the particles in each of these event halves. \mathbf{n}_z is a unit vector in the direction of the positron beam. If there are no particles in one of the event halves then ϕ_{acop} is set to 180° .

No event survived the cuts. The detection efficiency for $m_\chi = 21 \text{ GeV}$ was found to be 28%.

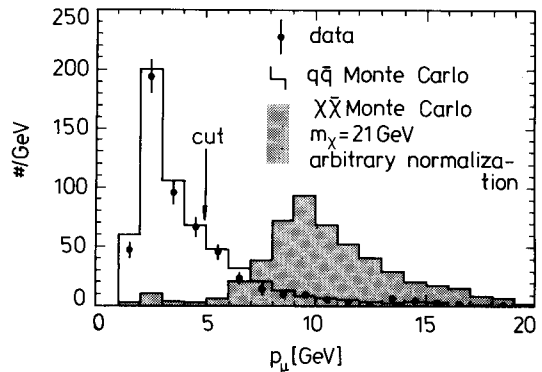


Fig. 5. Muon momenta p_μ

B) *Two jets, a muon + missing momentum.* The multihadron sample was used for this analysis.

1. A “good muon” selected with “loose” cuts and with momentum $p_\mu > 5$ GeV was required. In Fig. 5 the observed muon momentum spectrum is compared to that of a Monte Carlo simulation of multihadronic events [9]. Also shown is the expected distribution for leptoquark events, which is significantly different from that for ordinary multihadronic events.

2. $E_{\text{vis}} < \sqrt{s}$, as the events required contain neutrinos which escape detection.

3. $\phi_{\text{acol}} > 40^\circ \cdot (1 + 0.5 |\cos \theta_T|)$.

The acoplanarity angle

$$\phi_{\text{acol}} = \arccos \left(- \frac{\mathbf{p}_+ \cdot \mathbf{p}_-}{|\mathbf{p}_+| \cdot |\mathbf{p}_-|} \right) \quad (3)$$

is 180° minus the angle between the two momentum sum vectors defined above. Muons are not included in the momentum sums in order to treat them on an equal footing with the neutrinos in case A). As for the acoplanarity angle, the acoplanarity angle is defined to be 180° if all particles are in the same event half.

One event with an isolated muon in one event half opposite to a hadronic system in the other half survived these cuts. The event is shown in Fig. 6. It is consistent with background from $e^+ e^- \rightarrow q \bar{q} \mu^+ \mu^-$ in which one muon is not detected, or from the decay $D^\pm \rightarrow K^0 \mu^\pm \nu$ with an escaping K_L^0 . The detection efficiency for leptoquark events with $m_\chi = 21$ GeV is 50% after the above cuts have been applied.

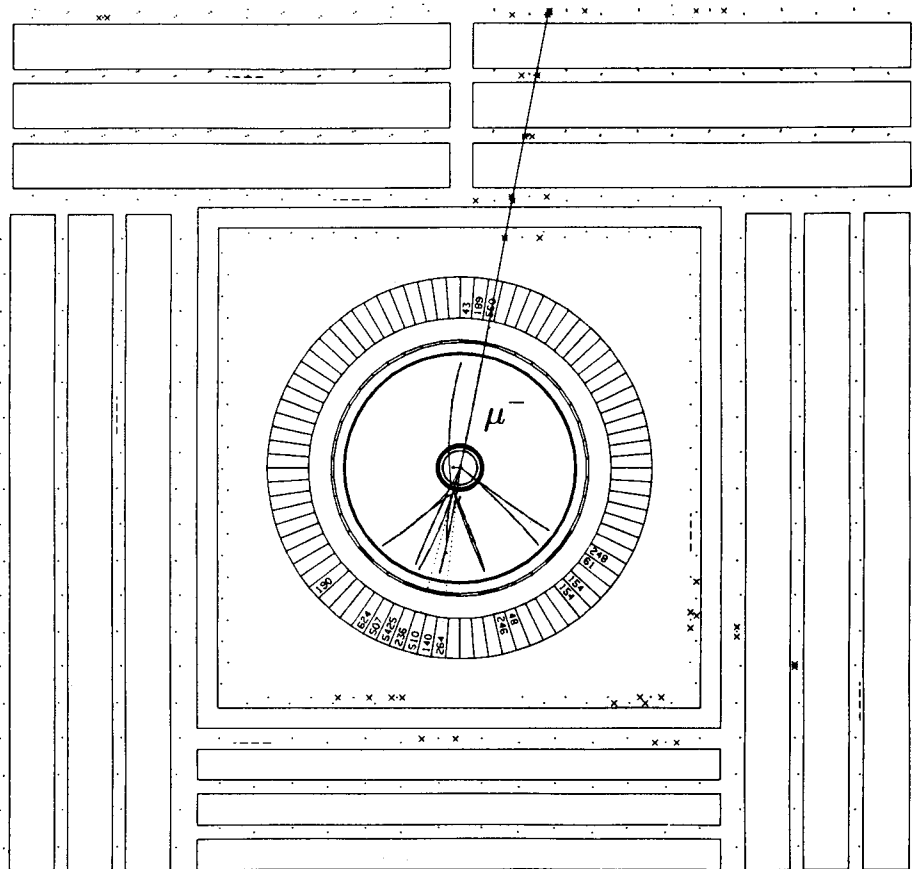
C) *Two jets + two muons.* The search for these events was performed on the multihadron sample, and the selection criteria were:

1. Two “good muons” (“loose” cuts) with momentum $p_\mu > 3$ GeV.

2. The transverse momentum with respect to the thrust axis (p_μ^T) was required to be larger than 5 GeV for at least one of the muons.

After these cuts the detection efficiency for $m_\chi = 21$ GeV is 44%. One event passes these cuts; it is event D from the low thrust – isolated muon analysis of Chap. 6 and is shown in Fig. 7. As the momentum of the second μ is too low to be associated with a high mass leptoquark decay, leptoquarks with $m_\chi > 16$ GeV cannot be the source of this event.

Fig. 6. Leptoquark candidate 1. The view along the beam axis shows the tracks of charged particles in the drift chamber, lead glass energies and hits in the muon filter. The centre of mass energy is 43.21 GeV and the muon has a momentum of 6.0 GeV. There is a nuclear interaction in the pressure vessel of the drift chamber, emitting a particle into the muon half. The charged particles alone, not counting those from the nuclear interaction, constitute an invariant mass of 3.9 GeV, thus excluding the possibility of this event being a τ -pair event



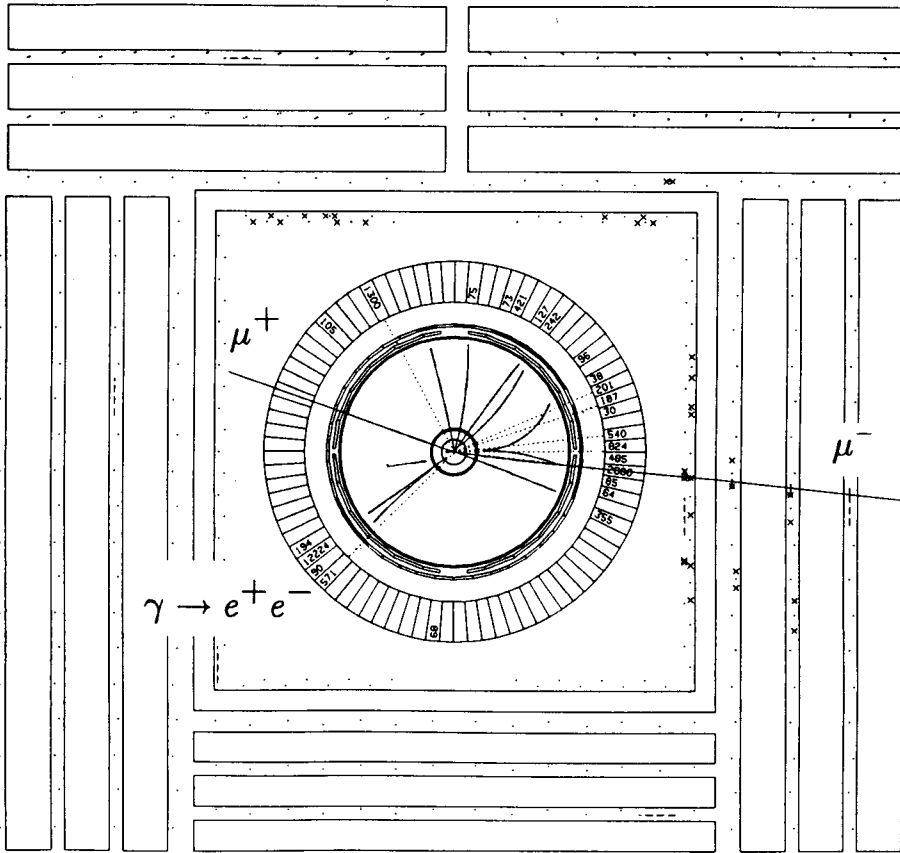


Fig. 7. Leptoquark candidate 2 (and event D from Chap. 6) at $\sqrt{s} = 46.57$ GeV. The momentum of the μ^+ is $21.8^{+18.2}_{-6.8}$ GeV, and that of the μ^- is 3.2 ± 0.3 GeV. The isolated converted photon has an energy of 14.4 GeV

4.3 Results

The detection efficiencies quoted are valid for leptoquark masses of 21 GeV. For lower masses they generally decrease and approach zero for masses below about 5 GeV.

Comparison of the number of candidate events to the number of expected leptoquark events, given the luminosity, cross section and detection efficiency, yields limits for the branching ratios and masses. The accepted events from cases B and C were taken as candidates; a background subtraction was not attempted.

Assuming second generation leptoquarks of charge $2/3$, which decay exclusively into second generation fermions, we obtain the bounds (95% C.L.) shown in Fig. 8 for the leptoquark mass and branching ratio $BR(\chi_\mu \rightarrow c \bar{\nu}_\mu) = 1 - BR(\chi_\mu \rightarrow s \mu^+)$. The combined limit from the analyses A), B) and C) excludes these leptoquarks from 5 GeV up to 20.8 GeV. The mass region below 5 GeV is not accessible to this analysis.

To account for leptoquarks of other charges and other decay channels, we also give limits in terms of $Q^2 \cdot BR(\chi \rightarrow q \nu) \cdot BR(\chi \rightarrow q \nu)$, $Q^2 BR(\chi$

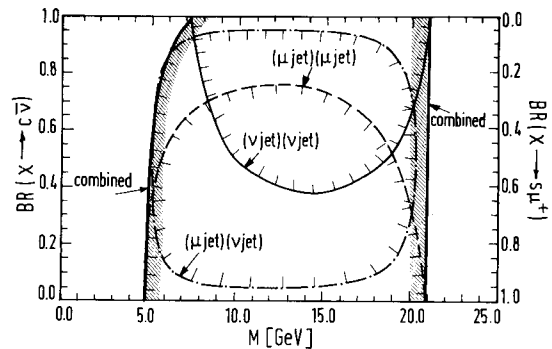


Fig. 8. Limits (95% C.L.) on mass and branching ratio $BR(\chi_\mu \rightarrow c \bar{\nu}_\mu)$ for second generation leptoquarks with charge $2/3$

$\rightarrow q \mu) \cdot BR(\chi \rightarrow q \nu)$ and $Q^2 \cdot BR(\chi \rightarrow q \mu) \cdot BR(\chi \rightarrow q \mu)$ in Fig. 9. These have been calculated assuming that the detection efficiencies are independent of quark flavor.

The lower mass limit of 20.8 GeV (95% C.L.) is not high enough to completely exclude a leptoquark interpretation of a $2\mu + 2$ jet event observed by the CELLO collaboration [15], which would suggest a leptoquark mass of about 20.5 GeV. Similar limits as in Fig. 8 were obtained by the CELLO collaboration [16].

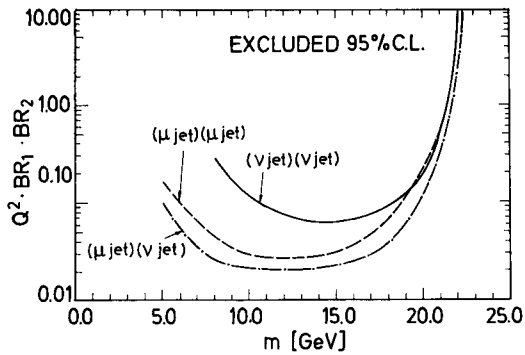


Fig. 9. Lower mass limits (95% C.L.) for leptoquarks of charge Q decaying into a quark and a muon or neutrino. BR_1 and BR_2 are the branching ratios of the leptoquarks

5 Chromoleptons

In some composite models [17, 18] color octet leptons l_8 may be sufficiently light to be produced at present accelerators. They decay into a gluon and their color singlet partner, the ordinary lepton. In e^+e^- annihilation, colored neutrinos, pair produced via a virtual Z^0 , would result in acoplanar jets, and colored muon pairs, mainly produced via a virtual photon at PETRA energies, in $2\mu+2$ jet events. The analysis of acoplanar jet events and dimuon events in the leptoquark search also puts limits on ν_8 and μ_8 .

For the pair production cross section σ_8 of colored leptons we assumed

$$\sigma_8 = 8 \cdot F(q^2) \cdot \sigma_1 \quad (4)$$

where 8 is the color factor, and $F(q^2)$ is a form factor to account for the compositeness of these objects; σ_1 is the cross section for the production of color singlet leptons.

Differences in quark and gluon fragmentation were neglected and it was assumed that the lifetime of the color octet particles is too short for these to

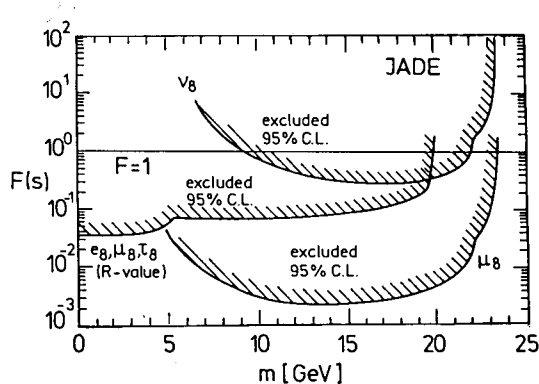


Fig. 10. Mass limits for chromoleptons. The limit from the measurement of the total hadronic cross section (R -value) is equally valid for e_8^\pm , μ_8^\pm and τ_8^\pm

Table 1. Summary of excluded mass regions for color octet leptons ($F(q^2)=1$)

	Lower limit	Upper limit	Analysis
l_8^\pm	0 GeV	19.8 GeV	R -value
e_8^\pm	0 GeV	$173 \text{ GeV} \cdot \lambda^{2/3}$	R -value
μ_8^\pm	5 GeV	23.2 GeV	hadronic dimuon events
ν_8	9 GeV	21.9 GeV	acoplanar jet events

be visible in the detector. With these assumptions the $\nu_8 \bar{\nu}_8$ and $\mu_8^+ \mu_8^-$ events look the same as the $c \bar{\nu}_\mu \bar{c} \nu_\mu$ and $s \mu^+ \bar{s} \mu^-$ events, with only the angular distributions for fermions (l_8) and bosons (χ) being different.

The resulting limits (95% C.L.) for the form factors and masses are given in Fig. 10. Charged chromoleptons would also contribute to the total hadronic cross section, and the limits derived from the R -value analysis [3, 6] are also shown. When $F=1$, which is expected since $q^2 = s \ll \Lambda_C^2$ (Λ_C is the compositeness scale) for PETRA energies (here $\langle s \rangle \approx 1900 \text{ GeV}^2$), the mass regions given in Table 1 can be excluded. A limit on color octet electrons previously published by JADE [6], where the effective coupling λ at the ee_8g vertex enters, is quoted for completeness.

6 Hadronic events

with low thrust containing isolated leptons

6.1 Introduction

All PETRA experiments have set bounds on new heavy quarks [19], from which open production of new charged $2/3$ quarks is excluded up to $m=23.3 \text{ GeV}$, and for charged $1/3$ quarks up to $m=22.7 \text{ GeV}$. Near threshold, events from heavy quarks would give rise to a spherical event topology, and leptons therein are expected to be produced by the semileptonic decays of the quarks.

Recently the Mark J group [1] reported the observation of an excess of muon inclusive hadronic events with low thrust

$$T = \max \frac{\sum_i |\mathbf{p}_i \cdot \mathbf{n}_T|}{\sum_i |\mathbf{p}_i|} \quad (5)$$

at the highest PETRA energies, $\sqrt{s} \geq 46.3 \text{ GeV}$, where the muon had a large isolation angle δ with respect

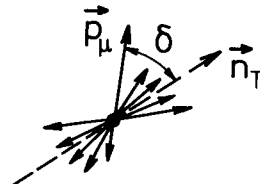


Fig. 11. Definition of isolation angle δ

to the thrust axis \mathbf{n}_T , as shown in Fig. 11. A search for this type of events within the JADE data sample of 22.8 pb^{-1} in the energy range 38.66 GeV to 46.3 GeV and 1.8 pb^{-1} between 46.3 GeV and 46.78 GeV is described in this chapter.

6.2 Inclusive muons

The analysed events were demanded to fulfill the multihadron conditions. Muons used in this chapter were required to satisfy the “loose” criteria as described in Sect. 2.2. In order to allow comparison of results, cuts identical to those used by Mark J were chosen to define the signal region, i.e. $T < 0.8$ and $|\cos \delta| < 0.7$. The results for $\sqrt{s} \geq 46.3 \text{ GeV}$ were compared to the expectation calculated from data with $\sqrt{s} < 46.3 \text{ GeV}$. In Fig. 12 the inclusive muon events are shown in the $T-|\cos \delta|$ plane for both of the centre of mass energy intervals, with the cuts indicated. The signal region for $\sqrt{s} \geq 46.3 \text{ GeV}$ contains five events compared to an expectation of (0.56 ± 0.18) events from an extrapolation of the lower energy data*. This expectation is in agreement with a Monte Carlo simulation of multihadron production with five flavors which predicts (0.74 ± 0.11) events in the signal region. The probability of a fluctuation of the observed magnitude (or larger) is less than 0.4%.

The energy flow of the five events, labelled A–E, at $\sqrt{s} \geq 46.3 \text{ GeV}$ with $T < 0.8$ and $|\cos \delta| < 0.7$, is shown in the plots of Fig. 13. In these diagrams the energy flow is rolled out in the $\cos \theta - \phi$ -plane, where θ is the polar angle with respect to the beam axis, and ϕ the azimuthal angle. Muons and electromagnetic showers with energies $E_{\text{e.m.}} > 5 \text{ GeV}$ are marked. Event D contains two muons and has already been shown in Fig. 7. We note the high muon momenta in events A and D and the energetic electromagnetic clusters, from either an electron or a photon in events A, D and E. Large electromagnetic clusters were also observed by Mark J in their excess events [21]. Except for event B, which is the candidate event with high transverse jet mass and a high p^T muon found previously in a heavy quark search [6], the events are planar, as can be seen from the Q -plots [22] attached to the legoplots. The visible energy and missing transverse momentum show no peculiarities when compared to ordinary multihadronic events.

In this analysis the standard muon criteria for new particle searches (“loose” cuts) were used, but only

* Recently we learnt that Mark J [20] did not include the muon when calculating the thrust, and that they did not balance the event before the calculation, as we do. Applying the Mark J procedure, we find a sixth event at $\sqrt{s} \geq 46.3 \text{ GeV}$, and the expectation changes slightly to 0.69 ± 0.21 .

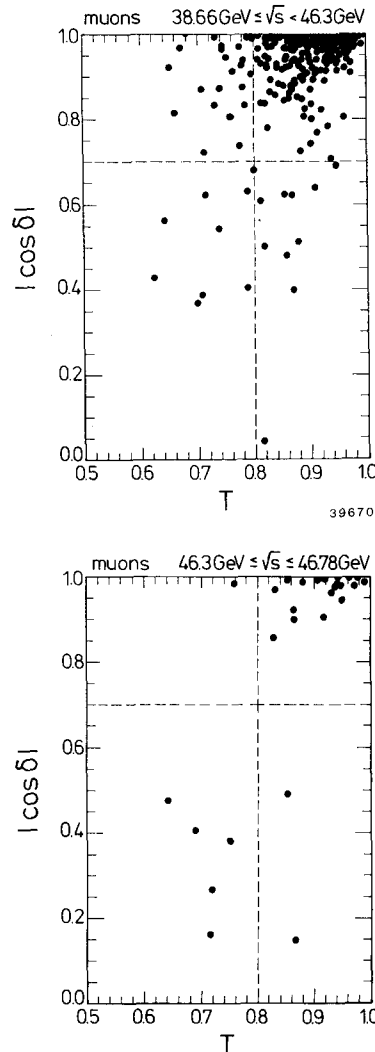


Fig. 12. T and $|\cos \delta|$ for muon inclusive events

two of the five muons fulfill the stricter requirements of the “tight” selection*. Two of the others hit regions of the muon filter with fewer chambers, where hadron rejection is reduced.

The observed excess might indicate the threshold of some new particle production above $\sqrt{s} = 46.3 \text{ GeV}$, and hence careful checks of the background were performed.

6.3 Background

Various tests have been carried out to check whether the observed events are due to an enhanced background of hadrons misidentified as muons at \sqrt{s}

* The second muon in event D and the muon in the sixth event, which appears when muons are not included in the thrust calculation, satisfy also the “tight” criteria

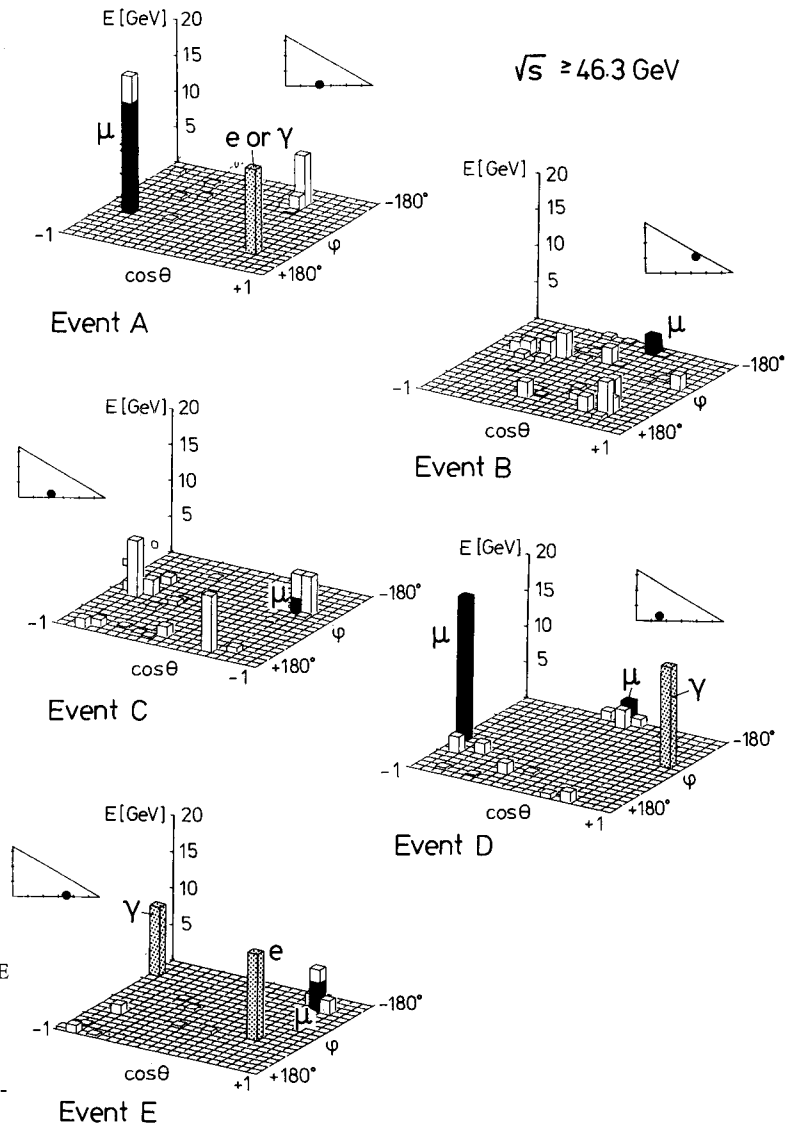


Fig. 13. Energy flow diagrams of the five μ -events A-E with $T < 0.8$ and $|\cos\delta| < 0.7$ at $\sqrt{s} \geq 46.3$ GeV. The corresponding Q-plots are also shown. Q_1, Q_2, Q_3 are the eigenvalues of the sphericity tensor, $(Q_3 - Q_2)/\sqrt{3}$ being plotted as abscissa and Q_1 as ordinate in the Q-plots

≥ 46.3 GeV as compared to $\sqrt{s} < 46.3$ GeV. A possible source of background is the increased emission of synchrotron radiation during the high energy scan, which caused spurious hits in the muon filter, especially in the forward region.

The fraction of events containing a muon for the two energy intervals agrees within errors, and also the angular distribution of the muons shows no significant excess over the entire polar range, as shown in Fig. 14.

The probability that a given hadron track with $p > 1.8$ GeV is classified as a muon can be determined from the data in the following way. The sample of observed tracks satisfying the muon selection criteria consists of prompt muons and fake muons. The

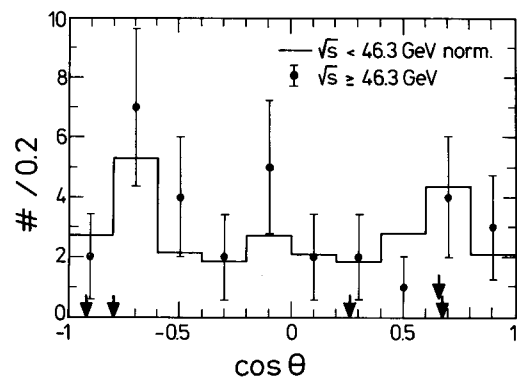


Fig. 14. Muon angular distribution; θ is the angle between the muon and the beam axis. The arrows mark the polar position of the five signal muons

prompt contribution is known from a Monte Carlo simulation, assuming that there are no new processes involved. The fake contribution is then the difference between the number of tracks satisfying the muon selection criteria and the prompt contribution. At the energy of interest, $\sqrt{s} \geq 46.3$ GeV, the fake probability was calculated to be $P_{h \rightarrow \mu} = (1.8 \pm 0.5)\%$. This number is in agreement with a measurement of the π punch-through+decay probability of $(1.5 \pm 0.3)\%$ using $\tau^+ \tau^-$ -pairs as a source of pion tracks.

In order to estimate the contribution of fake muons to the signal region, events with $T < 0.8$ and at least 1 track, irrespective of particle type, with $p > 1.8$ GeV and $|\cos \delta| < 0.7$ were selected at $\sqrt{s} \geq 46.3$ GeV. 30 events were found, containing in total 50 tracks fulfilling the above requirements. Assuming a probability of $P_{h \rightarrow \mu} = (1.8 \pm 0.5)\%$ as determined above to fake a muon, we estimate a background contribution of 0.90 ± 0.25 events to the observed signal of five events. This number is considered to be an upper limit, since most of the hadron tracks lie within jets, where the fake probability is larger than for the isolated tracks we are considering. From prompt muons, an additional 0.22 ± 0.03 events are expected in the signal region.

When the cut for the muon hit association to the jet chamber track is relaxed from 2σ to 5σ , we would expect a corresponding increase in the number of muons in the signal region, if they were due to random hits. Above 46.3 GeV no additional event was found in the signal region after relaxing the muon cut.

To summarize, though some of the muons do not belong to the cleanest sample, no indication was found that the five muon events are due to enhanced hadron contamination at $\sqrt{s} \geq 46.3$ GeV.

6.4 Inclusive electrons

The same multihadron data sample was searched for an excess of similar events with isolated electrons. For the electrons with $p > 1.8$ GeV we do not observe any event in the signal region ($T < 0.8$ and $|\cos \delta| < 0.7$) above 46.3 GeV, and expect 0.7 events from an extrapolation of the lower energy data (see Fig. 15). The electron in event E does not fulfill the quality requirements on the dE/dx measurement due to a nearby track. Another electron in event A is removed by the photon conversion cuts.

In ordinary multihadron events the detection efficiencies for electrons and muons coming from b - and c -decays are similar within the acceptance cut $|\cos \theta| < 0.76$. However, Monte Carlo studies have shown that multiparticle effects are more important for the detection of electrons than for muons. In particular for close tracks it may happen that an electro-

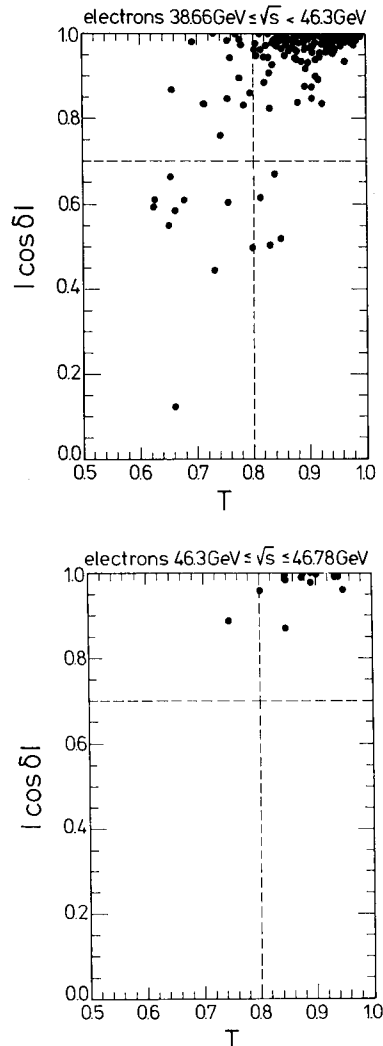


Fig. 15. T and $|\cos \delta|$ for electron inclusive events

magnetic shower cannot be uniquely assigned to one track. Such overlap problems are less severe in muon identification, where the presence of a muon would still be recognized in the muon filter. Therefore the electron detection efficiency is more strongly influenced by the special event topology caused by a possible new process.

In order to roughly estimate how many events with isolated electrons in a low thrust topology would correspond to the five observed muon events, the muon tracks in these events were replaced by electrons, and the electron selection criteria were applied. Two of the replaced muons are outside the electron acceptance $|\cos \theta| < 0.76$, two others have a high probability of escaping detection due to nearby particles, and one event has a similar detection probability as either an electron or a muon event. These studies imply that the absence of electron events in our present data does not contradict lepton universality.

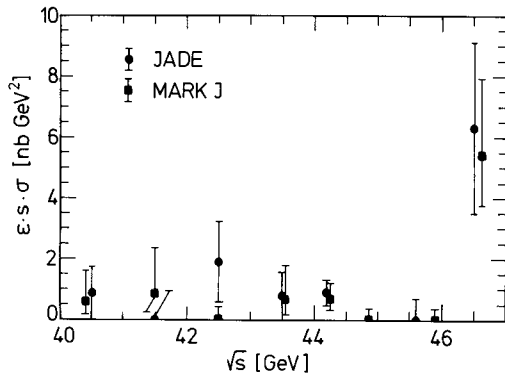


Fig. 16. Cross section for muon events with $T < 0.8$ and $|\cos \delta| < 0.7$. The error bars are shown to give a feeling for possible fluctuations; for such low statistics they cannot be used to calculate significances in terms of standard deviations

6.5 Comparison with other experiments

The cross section for inclusive muon events with $T < 0.8$ and $|\cos \delta| < 0.7$ is plotted as a function of the centre of mass energy in Fig. 16 and compared with the result of Mark J [21]. The data are not corrected for acceptance. Both experiments, Mark J and JADE, observe an excess in the highest energy bin. Mark J sees seven events and expects 0.5 in its data sample of 2.8 pb^{-1} .

CELLO [23] does not confirm this observation, observing one event at $\sqrt{s} \geq 46.3 \text{ GeV}$ with an integrated luminosity of 2.1 pb^{-1} . Below 46.3 GeV the rates measured by CELLO agree with those of Mark J and JADE. CELLO's detection efficiency for the events observed by Mark J and JADE was found to be comparable to that of JADE and Mark J [23, 20].

7 Summary

A search for rare processes leading to events containing hadrons and muons or missing energy was conducted. Three events of the type two isolated muons + hadrons have been observed. The rate and their kinematic configurations agree with the QED expectation for the reaction $e^+ e^- \rightarrow q \bar{q} \mu^+ \mu^-$.

Leptoquarks of the second generation are excluded in the mass range 5 GeV up to 20.8 GeV , color octet muons up to 23.2 GeV and color octet neutrinos from 9 GeV up to 21.9 GeV .

At the highest PETRA energies, $46.30 \text{ GeV} \leq \sqrt{s} \leq 46.78 \text{ GeV}$, five low thrust events with isolated muons were observed, whereas only 0.56 ± 0.18 events were expected from an extrapolation from lower energies. No satisfactory explanation for this excess in terms of background could be found. Similar observations were made by Mark J, while CELLO does not

observe this effect. Events from a new heavy quark, e.g. a charged $1/3$ quark of the fourth generation [24], which cannot yet be excluded by PETRA, are expected to be more spherical than most of the five observed events. With the close down of PETRA, it is left to experiments at TRISTAN to determine whether these events indicate more than a statistical fluctuation.

Acknowledgements. We are indebted to the PETRA machine group and the DESY computer centre staff for their excellent support during the experiment and to the engineers and technicians of the collaborating institutions who have participated in the construction and maintenance of the apparatus. We thank J. Fuster of the CELLO group and B. Wyslouch of the Mark J Group for their cooperation, and B. Schrempp, F. Schrempp and K. Hagiwara for helpful discussions. This experiment was supported by the Bundesministerium für Forschung und Technologie, by the Ministry of Education, Science and Culture of Japan, by the UK Science and Engineering Research Council through the Rutherford Appleton Laboratory and by the US Department of Energy. The visiting groups at DESY wish to thank the DESY directorate for the hospitality extended to them.

References

1. Mark J Collab. B. Adeva et al.: Phys. Rev. D 34 (1986) 681
2. JADE Collab. W. Bartel et al.: Phys. Lett. 88 B (1979) 171; B. Naroska: Phys. Rep. 148 (1987) 67
3. JADE Collab. W. Bartel et al.: Phys. Lett. 129 B (1983) 145
4. J. Allison et al.: Nucl. Instrum. Methods A 238 (1985) 220
5. J. Allison et al.: Nucl. Instrum. Methods A 238 (1985) 230
6. JADE Collab. W. Bartel et al.: Phys. Lett. 160 B (1985) 337
7. JADE Collab. W. Bartel et al.: Z. Phys. C - Particles and Fields 33 (1987) 339
8. F.A. Berends, P.H. Daverfeldt, R. Kleiss: Phys. Lett. 148 B (1984) 489; Nucl. Phys. B 253 (1985) 441
9. B. Anderson, G. Gustafson, T. Sjöstrand: Phys. Lett. 94 B (1980) 243; T. Sjöstrand: Comput. Phys. Commun. 27 (1982) 105
10. B. Schrempp, F. Schrempp: Phys. Lett. 153 B (1985) 101
11. R.N. Mohapatra, G. Segrè, L. Wolfenstein: Phys. Lett. 145 B (1984) 433
12. C. Peterson et al.: Phys. Rev. D 27 (1983) 105
13. JADE Collab. W. Bartel et al.: Phys. Lett. 146 B (1984) 126
14. JADE Collab. W. Bartel et al.: Phys. Lett. 155 B (1985) 288
15. CELLO Collab. H.-J. Behrend et al.: Phys. Lett. 141 B (1984) 217
16. CELLO Collab. H.-J. Behrend et al.: Phys. Lett. 178 B (1986) 452
17. H. Harari: Phys. Lett. 156 B (1985) 250; H. Harari: Report WIS-85/6 Ph-Feb. WIS-85/16 Ph-March and WIS-85/23 Ph-June, Weizman Institute of Science, Rehovot 1985
18. S.F. King, S.R. Sharpe: Nucl. Phys. B 253 (1985) 1
19. S. Komamiya: Proc. of the 1985 International Symposium on Lepton and Photon Interactions, Kyoto 1985
20. Mark J Collab. B. Wyslouch: private communication
21. A. Böhm: Proc. of the XXth Rencontre de Moriond, Les Arcs 1985/1, 559
22. JADE Collab. W. Bartel et al.: Z. Phys. C - Particles and Fields 21 (1983) 37
23. CELLO Collab. H.-J. Behrend et al.: DESY 87-016, Hamburg 1987
24. F. Cornet, E.W.N. Glover, K. Hagiwara, A.D. Martin, D. Zepfenfeld: Phys. Lett. 174 B (1986) 224; V. Barger, R.J.N. Phillips, A. Soni: Phys. Rev. Lett. 57 (1986) 1518